

# Synergistic effect of water soluble chitin and iodide ion on the corrosion inhibition of mild steel in acid medium

Yesodaran Sangeetha<sup>1</sup>, Sankaran Meenakshi<sup>1</sup>, Chandrasekaran Sairam Sundaram<sup>2\*</sup>

<sup>1</sup>Department of Chemistry, The Gandhigram Rural Institute – Deemed University, Gandhigram, Tamil Nadu, 624 302, India

<sup>2</sup>Department of Science and Humanities, Women's Polytechnic College, Lawspet, Puducherry, 605008, India

\*Corresponding author. Tel: (+91) 413-2252833; E-mail: [sairam\\_adithya@yahoo.com](mailto:sairam_adithya@yahoo.com)

Received: 24 November 2015, Revised: 16 December 2015 and Accepted: 22 May 2016

## ABSTRACT

The inhibition performance of water soluble chitin (WSC) and its synergistic inhibition with potassium iodide (KI) in 1 M HCl was studied using gravimetric and electrochemical measurements. From gravimetric measurement it is inferred that there is an increase in inhibition efficiency with the increased addition of inhibitor and it further stepped up to a higher value in the presence of 0.1 % KI. Polarization studies revealed that there is mixed mode of inhibition by WSC. Impedance study suggested the adsorption of the inhibitor at the interface between mild steel and acidic solution. The adsorption of inhibitor followed Frumkin isotherm. Scanning Electron Microscopy (SEM) and Energy Dispersive X-ray (EDX) confirmed the co-adsorption of KI with WSC on the mild steel surface. Fourier Transform Infra-red (FTIR), Atomic Force Microscopy (AFM) and X-ray Diffraction (XRD) indicated the formation of protective film by the inhibitor on the surface of mild steel. Copyright © 2016 VBRI Press.

**Keywords:** Mild steel; chitin; acid corrosion; FTIR; AFM.

## Introduction

Metals and alloys have been deployed in industrial sector as a material for constructing reaction vessels, storage tanks, etc. Mild steel is one such alloy employed widely in industries due to low cost and good mechanical strength. During acid cleaning, descaling and oil well acidizing, the mild steel surface is exploited by the menace, corrosion in the acidic condition. Hence, corrosion inhibition of mild steel has been studied in the present work. The addition of small amount of corrosion inhibitors in the solution secures the metal from aggressive medium at the metal/solution interface. Corrosion inhibitors have been most widely used and their global market has been expected to be around \$ 6 million in 2015 [1]. The rate of metal dissolution was reduced by inorganic inhibitors like phosphates, chromates, tungstates and molybdates through the oxidation of the metal surface. The organic compounds, particularly heterocyclic compounds were reported as efficient corrosion inhibitors for mild steel [2-5]. The compounds containing nitrogen were found to be effective inhibitors for mild steel in hydrochloric acid medium. The toxicity and high cost of these inhibitors restricts their application.

In the recent past, the research in corrosion inhibition has been geared towards natural, non-toxic, renewable and inexpensive materials. Several natural products like plant extracts [6, 7], vegetables [8, 9], fruits [10, 11], guar gum [12], starch [13], tannin [14], cellulose derivatives [15-17], pectin [18] and chitosan derivatives [19-23], have been reported in the literature as efficient corrosion inhibitors.

These materials are available in abundance and are biodegradable in nature. The veracity of these inhibitors, particularly biopolymers are high due to their high chelating ability with metals. Fruitful endeavours have been experienced by scientists in their effort to combat corrosion in mild steel using derivatives of biopolymers like cellulose and chitosan [24]. Umoren et al., have reported that the inhibition efficiency of chitosan on mild steel in HCl as 68 % [25]. Chitosan is fully or partially deacetylated product of chitin. Chitin is the second most abundant material next to cellulose. Hence chitin or chitosan can be applied as corrosion inhibitors by increasing the inhibition efficiency.

Chitin, a biopolymer is a natural amino polysaccharide with a unique structure, biocompatible and biodegradable in nature. This polymer is made up of  $\beta$ - (1-4)-2-acetamido-2-deoxy- $\beta$ -D-glucose units. In the present work, inhibition efficiency of water soluble chitin has been improved by adding iodide. The synergism of chitin with iodide ion on mild steel has been evaluated using chemical (weight loss) and electrochemical (polarization and electrochemical impedance spectroscopy) methods. The adsorbed film was characterized with Fourier Transform Infrared spectroscopy (FTIR) and X-ray Diffraction (XRD) methods. The surface morphology study was carried out using Atomic Force Microscopy (AFM) analysis. The effect of addition of KI was studied using weight loss, polarization studies, impedance method and Scanning Electron Microscope (SEM).

## Experimental

### Materials

The mild steel used in this investigation has the following chemical composition (wt%): C 0.096, Si 0.062, Mn 1.499, S 0.014, Cr 0.015, P 0.013, Cu 0.033 and balance Fe. The steel sample was press cut into coupons of dimensions  $3.5 \times 1.5 \times 0.04$  cm and used for immersion in the weight loss studies. The working electrode used in electrochemical methods has an exposed surface area of  $1 \text{ cm}^2$ . The other portions of the working electrode were covered with epoxy resin. The steel specimens were polished with silicon carbide papers (320, 600, 800, 1000 and 1200 grit), washed with double distilled water, degreased with acetone and dried in warm air. Water soluble chitin (WSC) with degree of acetylation 55 % was purchased from Pelican Biotech and Chemicals lab, Kerala (India). Analytical grade hydrochloric acid was used for preparing aggressive solution. Potassium iodide was purchased from central drug house, New Delhi. The structure of chitin has been shown in **Fig. S1** (supporting information).

### Weight loss method

Gravimetric measurements were carried out as described elsewhere [20]. In brief, rectangular mild steel coupons in triplicate were suspended in 100 mL of 1 M HCl, in the absence and presence of different concentrations of the inhibitor. Experiments were carried out in the static condition, at room temperature. After a period of immersion of 2 h, the coupons were withdrawn, washed using bidistilled water and dried at room temperature. The differences in weight, before and after the immersion were calculated. The average of weight loss of the three measurements was taken. The effect of temperature on the inhibition of WSC was studied in the temperature range 303 K – 323 K. The inhibition efficiency was calculated using the equation 1.

$$IE (\%) = \frac{W_0 - W_1}{W_0} \times 100 \quad (1)$$

$W_0$  and  $W_1$  represent the weight loss of the mild steel specimens observed without and with different concentrations of the inhibitor. The addition of 0.1 % KI to 500 ppm of the inhibited solution was also carried out.

### Electrochemical measurements

The working electrode was the mild steel specimen with an exposed surface area of  $1 \text{ cm}^2$ . The platinum electrode acted as the counter electrode. The saturated calomel electrode (SCE) was taken as the reference electrode. All the potentials were expressed with respect to SCE. Measurements were carried out in unstirred condition, in open air using the CHI Electrochemical analyzer (model 760 D) with an operating software CHI 760D. Steady state potential was obtained before each measurement, by immersing the working electrode in the test solution for 30 minutes. Polarization curves were recorded between the potential range -300 mV to +300 mV vs SCE, at a scan rate of 1 mV/sec. Extrapolation of the tafel curves gives the

value of corrosion current density  $I_{\text{corr}}$  and corrosion potential  $E_{\text{corr}}$ .

Electrochemical impedance measurements (EIS) were performed in the frequency range 10 kHz to 100 mHz, with an amplitude of 5 mV peak to peak, at open circuit potential. The value of charge transfer resistance  $R_{\text{ct}}$  and capacitance of double layer  $C_{\text{dl}}$  can be obtained from the Nyquist plot. The effect of addition of 0.1 % KI to the inhibitor was studied using the polarization and impedance methods.

### Fourier transform infra-red (FTIR)

FTIR analysis was performed with FT-IR JASCO 460 plus model instrument, in the frequency range  $4000 - 400 \text{ cm}^{-1}$ . After an immersion period of 2 h the steel coupon was removed from the test solution containing 500 ppm of inhibitor, dried and the adsorbed film was scraped from the surface using a knife. Then, IR spectra of WSC and WSC adsorbed on mild steel surface were recorded.

### Surface analysis

The morphology of the uninhibited and inhibited mild steel sample was studied using SEM (VEGA3TESCAN fitted with Bruker Nano GmbH, Germany) and AFM (NanoSurf Easyscan2 instrument, USA model). The specimen with the dimension  $3.5 \times 1.5 \times 0.04$  cm was used for SEM analysis and another with  $1 \times 1$  cm dimension was utilised for AFM measurement.

Measurements for both the methods were carried out after immersion for a period of 2 h in the test solution without and with 500 ppm of inhibitor. The effect of addition of 0.1 % KI was studied using SEM and energy dispersive X-ray (EDX).

### X-ray diffraction (XRD) study

X-ray diffraction analysis of the WSC and WSC adsorbed on the mild steel surface containing 500 ppm inhibitor (Removed as per the procedure given) were carried out using X' per PRO model with PANalytical make diffractometer. The measurements were made in the angle range  $10^\circ < 2\theta < 80^\circ$ .

**Table 1.** Corrosion parameters obtained from weight loss of mild steel in 1M HCl in the absence and presence of different concentrations of WSC and WSC + KI at room temperature.

Concentration (ppm)	CR ( $\text{mg cm}^{-2} \text{ h}^{-1}$ )	IE (%)
Blank	3.05	-
100	2.21	27.5
200	1.82	40.2
300	1.31	57
400	0.82	73
500	0.61	79.9
500+0.1% KI	0.20	90.5

## Results and discussion

### Weight loss measurement

The rates of corrosion and the inhibition efficiency of WSC on mild steel immersed in 1 M HCl in the absence and presence of various concentrations of the inhibitor were

studied and the data were compiled in **Table 1**. The corrosion rate (CR) decreased and the inhibition efficiency (IE) increased with the increased addition of the inhibitor. On scrutinising the **Table 1**, it is inferred that there is a prominent increase in the inhibition efficiency (90.5 %) on addition of WSC and KI to the aggressive solution. This could be due to the synergistic effect of KI exerted on inhibition effect of WSC.

#### Adsorption isotherm

The primary step in the inhibition of corrosion is the adsorption of the inhibitor on the surface of the metal to be protected. Thus, the study of nature of adsorption became quiet essential in getting an insight into the mechanism of inhibition. The degree of surface coverage ( $\theta$ ) was obtained from the weight loss results and fitted with various adsorption isotherms. The best fit was obtained with Frumkin isotherm (**Fig. S2**) containing the following equation:

$$\log \left\{ [C] \times \frac{\theta}{1-\theta} \right\} = 2.303 \log K + 2\alpha\theta \quad (2)$$

where, C represents concentration,  $\theta$  the surface coverage,  $\alpha$  the interaction parameter and K denotes the adsorption-desorption equilibrium constant and it is related to the standard free energy of adsorption by the equation:

$$K = \frac{1}{55.5} \exp \left( \frac{-\Delta G_{\text{ads}}^{\circ}}{RT} \right) \quad (3)$$

where, 55.5 indicates the concentration of water in mol dm<sup>-3</sup>, R the molar gas constant and T the absolute temperature. The  $\Delta G$  values obtained were between -14 kJ/mol to -15 kJ/mol (**Table S1**) and the regression coefficient ( $R^2$ ) was above 0.99.  $\Delta G$  values below 20 kJ/mol suggest physisorption of the inhibitor on the mild steel surface. Further,  $\Delta G$  values decreased (becomes more negative) with increase in temperature which indicates the endothermic nature of the adsorption process.

#### Polarization method

The electrochemical parameters like corrosion potential ( $E_{\text{corr}}$ ), corrosion current ( $I_{\text{corr}}$ ), anodic tafel slope ( $\beta_a$ ) and cathodic tafel slope ( $\beta_c$ ) were calculated from tafel extrapolation and given in **Table 2**. The corresponding tafel curves have been depicted in **Fig. 1**. The percentage of inhibition was determined from  $I_{\text{corr}}$ , using equation 4.

$$\text{IE (\%)} = \frac{I_{\text{corr}}^{\circ} - I'_{\text{corr}}}{I_{\text{corr}}^{\circ}} \times 100 \quad (4)$$

where,  $I_{\text{corr}}^{\circ}$  and  $I'_{\text{corr}}$  denote the corrosion current densities without and with different concentrations of the inhibitor, respectively. The current density is reduced from 799  $\mu\text{A}/\text{cm}^2$  for the blank solution, to 78.8  $\mu\text{A}/\text{cm}^2$  for the solution containing 500 ppm of inhibitor. The reduction in current density is evident even for the lowest concentration of the inhibitor and it is more pronounced at the optimum concentration (500 ppm) of the WSC.

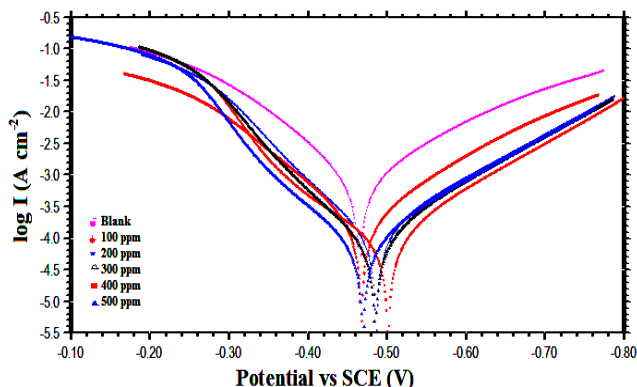


**Fig. 1.** Tafel curves for mild steel in 1 M HCl containing different concentrations of WSC.

The  $E_{\text{corr}}$  is found to be shifted towards negative direction from the value of uninhibited solution. Maximum displacement in  $E_{\text{corr}}$  is around 36 mV. The compound can be considered as anodic or cathodic inhibitor only when the change in  $E_{\text{corr}}$  is more than 85 mV [26]. Thus, we may conclude that the performance of the inhibitor as mixed type of inhibition. Both anodic and cathodic tafel slopes have been altered with the addition of the inhibitor. This indicates that both metal dissolution reaction at anode and hydrogen evolution reaction at cathode are affected by the addition of WSC. The maximum inhibition efficiency (IE) is 78.6 %, which suggested that the inhibitor is adsorbed on the surface of mild steel, forming a barrier film between the metal and the acidic solution.

**Table 2.** Polarization parameters from tafel plots for the corrosion of mild steel in 1 M HCl containing different concentrations of WSC and WSC + KI.

Concentration (ppm)	$E_{\text{corr}}$ (mV)	$I_{\text{corr}}$ ( $\mu\text{A}/\text{cm}^2$ )	$\beta_c$ (mV/dec)	$\beta_a$ (mV/dec)	IE (%)
Blank	-466	369	133.3	100.1	-
100	-487	193	133.5	83.7	47.7
200	-467	180.7	120.9	97.1	51
300	-502	94.4	124.3	112.8	74.4
400	-485	84.5	125.7	81.7	77.1
500	-470	78.8	126.6	90.7	78.6
500 + 0.1%KI	-487	26.8	87.2	89.3	92.7

#### Impedance parameters

Nyquist plots (**Fig. 2**) represent the impedance measurements carried out at open circuit potential after 30 minutes of immersion in 1 M HCl solution without and with inhibitor. There was only a single capacitive loop at high frequency, suggesting one time constant in bode plots. The Nyquist diagrams were not perfect semi circles which could be attributed to the inhomogeneties generally found on the solid electrode and frequency dispersion [27]. The difference in impedance at the lower and higher frequencies in the plot represents the charge transfer resistance ( $R_{\text{ct}}$ ). The inhibition efficiency (IE) was calculated using the following equation:

$$\text{IE (\%)} = \frac{R_{\text{ct}} - R'_{\text{ct}}}{R_{\text{ct}}} \times 100 \quad (5)$$

where,  $R_{\text{ct}}$  and  $R'_{\text{ct}}$  denote the charge transfer resistance values in the presence and in absence of different concentrations of the inhibitor, respectively. The

capacitance of double layer ( $C_{dl}$ ),  $R_{ct}$  and the inhibition efficiency were calculated and enumerated in **Table S2**. The decrease in  $C_{dl}$  at the mild steel acid solution interface indicated the decrease in local dielectric constant and/or an increase in thickness of the electrical double layer. There is a pronounced increase in  $R_{ct}$  value on moving from lower to higher concentration of WSC. This is due to the formation of a protective film by the inhibitor at the metal/solution interface. A maximum inhibition efficiency of about 83.5 % is obtained for the optimum concentration (500 ppm).

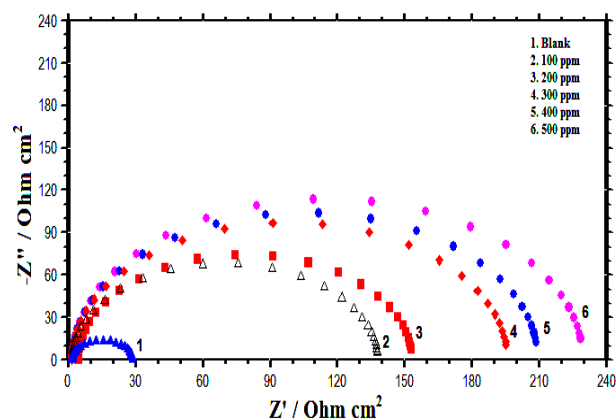


**Fig. 2.** Impedance diagrams for mild steel in 1 M HCl containing different concentrations of WSC.

#### FTIR analysis

The FTIR spectra of WSC and WSC adsorbed on mild steel were taken and enumerated in **Fig. 3** [28]. The chitin sample showed peaks at  $3437\text{ cm}^{-1}$  (-OH and -NH stretching vibrations including hydrogen bond), at  $2922\text{ cm}^{-1}$  (-CH<sub>2</sub> asymmetric stretching), doublet at  $1657\text{ cm}^{-1}$  and  $1623\text{ cm}^{-1}$  corresponding to amide I, at  $1557\text{ cm}^{-1}$  (amine group), at  $1316\text{ cm}^{-1}$  (amide III) and a ring stretching frequency at  $894\text{ cm}^{-1}$ .

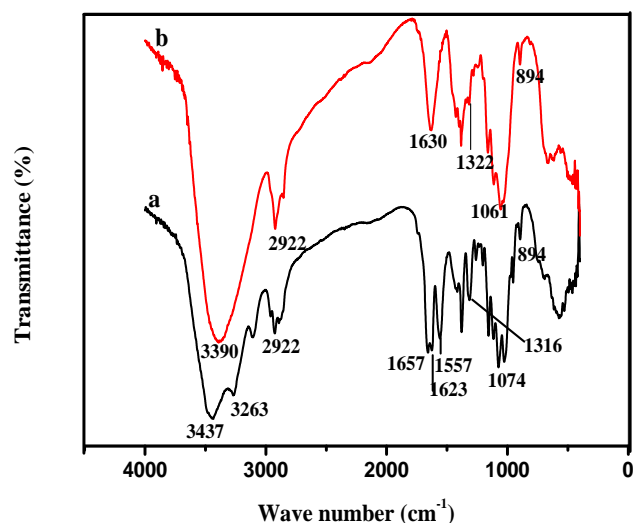


**Fig. 3.** FTIR spectra of (a) WSC and (b) WSC adsorbed on mild steel.

In curve b, corresponding to the adsorbed film, the -OH and -NH group bands have been shifted to  $3390\text{ cm}^{-1}$ . Peak

corresponding to -CH<sub>2</sub> is present in the adsorbed film ( $2922\text{ cm}^{-1}$ ). Amide I doublet is shifted to  $1630\text{ cm}^{-1}$  as single peak. The peak corresponding to amine ( $1557\text{ cm}^{-1}$ ) disappeared. Amide III band is shifted to  $1322\text{ cm}^{-1}$ . The peak corresponding to C-O-C band ( $1072\text{ cm}^{-1}$ ) is shifted to  $1061\text{ cm}^{-1}$ . Thus -OH, -NH and oxygen may have electrostatic interaction with the mild steel surface, which gives rise to shift in their peaks.

#### XRD analysis

The X-ray diffraction pattern of the water-soluble chitin (**Fig. S3**) shows peaks at  $2\theta$  values of 12.82, 19.4, 20.7, 26.3, and 39.2. The standard  $2\theta$  values of  $\alpha$ -chitin as given by Cho et al. [29], are 9.1 (020), 19.2 (110, 040), 20.03 (101), 23.11 (130) and 26.25 (013). We see that there has been a shift in the peak values of water-soluble chitin, which showed that there has been slight distortion in the orthorhombic structure with loosening in compactness. This less compact structure helped the water molecules diffuse into the compound easily. This fact confirmed its water soluble nature. In the curve 'b', where chitin is adsorbed on mild steel, the peaks are slightly shifted to  $23.32^\circ$  and  $26.62^\circ$ . No peak appeared around  $19^\circ$ . Peaks at  $51.97^\circ$  and  $67.32^\circ$  correspond to iron oxide and iron respectively. The peaks corresponding to chitin have appeared with slight shift. Thus XRD confirmed the adsorption of chitin on mild steel surface.

#### AFM analysis

The three dimensional images of the specimens immersed in uninhibited and inhibited solution for 2 h were obtained from the AFM analysis and given in **Fig. S4**. The roughness of the inhibited specimen has been reduced after the addition of 500 ppm of inhibitor. The roughness factor ( $S_a$ ) for the mild steel sample immersed in 1 M HCl without and with inhibitor are 136.6 nm and 98 nm respectively.

#### Synergistic effect of iodide and WSC

The effect of iodide ions on the inhibition of WSC on mild steel in 1 M HCl was assessed by gravimetry, polarization and impedance studies. The iodide ions exhibited comparatively better synergism than the other halide ions because, it has larger ionic radius. High hydrophobicity and low electronegativity are the other characteristics of this ion [30]. The addition of 0.1 % KI to 500 ppm of inhibitor in the acidic solution increased the inhibition efficiency from 83.7 % to 90.5 %. The I<sup>-</sup> ions competed with Cl<sup>-</sup> ions for adsorption on the surface of mild steel. After adsorption of iodide ions, the positively charged inhibitor ions are dragged into the double layer by electrostatic interaction with the adsorbed iodide ions [31].



where,  $I_{\text{sol}}$  and  $I_{\text{ads}}$  represents the iodide ion in the solution and iodide ion adsorbed on mild steel respectively.  $\text{Inh}_{\text{sol}}$  represent the inhibitor in solution. The  $(I - \text{Inh})_{\text{ads}}$  represents ion-pair of iodide and inhibitor adsorbed on steel

surface. A smooth surface appeared in SEM analysis for the specimen immersed in HCl solution containing KI and WSC (Fig. 4 a, b and c). The adsorption of iodide ions is confirmed with energy dispersive X-ray (EDX), which has been shown in Fig. S5.

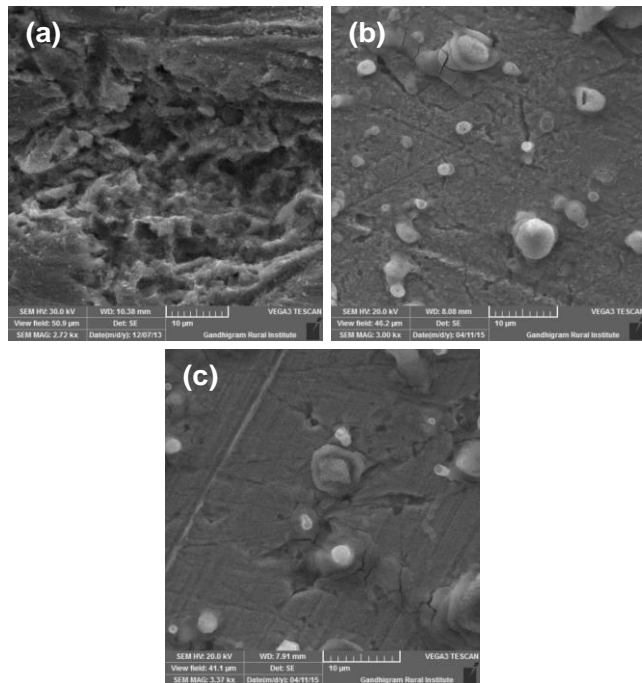


**Fig. 4.** SEM images of mild steel in (a) 1 M HCl (b) 500 ppm WSC (c) 500 ppm WSC + 0.1 % KI.

The polarization behaviour of mild steel in the presence of 0.1 % KI and 500 ppm inhibitor has been depicted in Fig. 5a and the parameters in Table 2. Both anodic and cathodic curves are changed and the decrease in current density is prominent. The  $E_{\text{corr}}$  has been shifted to the negative region. In the anodic region, there is desorption of the inhibitor from metal surface at a potential above -400 mV vs SCE. This potential has been usually referred to as desorption potential. The inhibition efficiency is stepped up to 92.7 % from 78.6 % (optimum concentration of WSC).

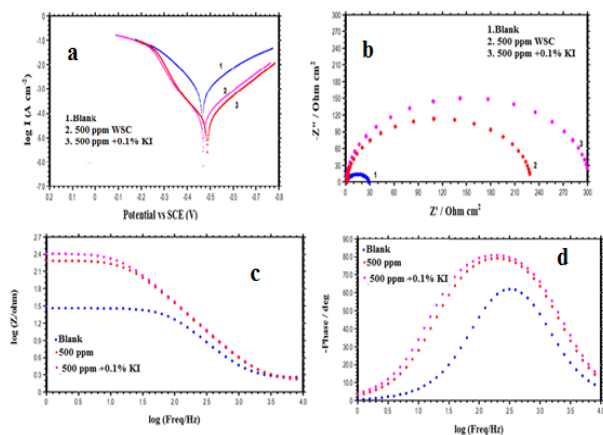


**Fig. 5.** (a) Tafel curves of mild steel in 1 M HCl in the absence and presence of WSC + KI (b) Nyquist, (c and d) Bode plots of mild steel in 1 M HCl in the absence and presence of WSC + KI.

The Nyquist and Bode plots for the inhibition of mild steel by WSC in the presence of 0.1 % KI has been

depicted in Fig. 5 b, c and d. The charge transfer resistance ( $R_{\text{ct}}$ ) has been increased from  $228.9 \Omega \text{ cm}^2$  to  $301 \Omega \text{ cm}^2$  in the presence of iodide ion, resulting in an improved inhibition efficiency of 90.9 % from 83.5 % for the optimum concentration of inhibitor. There has been a considerable decrease in double layer capacitance ( $C_{\text{dl}}$ ) from  $551 \mu\text{F}/\text{cm}^2$  for the blank solution to  $4.6 \mu\text{F}/\text{cm}^2$  in the presence of WSC and KI. This effect has been attributed to the synergistic inhibition between KI and WSC. There is an increase in phase angle in the Bode plot. There has been a good coherence between the results obtained in weight loss method and impedance measurement.

## Conclusion

WSC was found to be an effective inhibitor for mild steel in 1 M HCl. Chemical and electrochemical studies revealed an increase in the inhibition efficiency with the increase in concentration of the inhibitor. There is physisorption of inhibitor on the mild steel surface and the adsorption followed Frumkin isotherm. WSC exhibited mixed mode of inhibition. Impedance parameters suggested the adsorption of inhibitor. FTIR, SEM and AFM confirmed the adsorption of the inhibitor. XRD measurements indicated the presence of WSC on mild steel surface. The synergistic effect of iodide ion in combination with WSC due to co-adsorption is proved by weight loss, polarization and impedance studies. There is a considerable increase in inhibition efficiency of WSC on addition of KI. The veracity of this fact is ascertained with EDX analysis. SEM images clearly indicated the presence of adsorbed species (WSC and I) and a smooth surface.

## Reference

1. Yoo, SH.; Kim, YW.; Chung, K.; Baik, SY.; Kim, JS. *Corros. Sci.* **2012**, *59*, 42.
2. Granese, SL. *Corrosion*. **1988**, *44*, 322.
3. Bentiss, F.; Lagrenee, M.; Traisnel, M.; Hornez, JC. *Corros. Sci.*, **1999**, *41*, 789.
4. Bentiss, F.; Lagrenee, M.; Traisnel, M.; Mernari, B.; Elattari, H. *J. Appl. Electrochem.* **1999**, *29*, 1073.
5. Tadros, AB.; Abd-el-Nabey, BA. *J. Electroanal. Chem. Interfac.* **1988**, *246*, 433.
6. Ramesh, SP.; Vinod Kumar, KP.; and Sethuraman, MG. *Bull. Electrochem.* **2001**, *17*, 141.
7. Loto, CA. *Corros. Prevent. Contr.* **2001**, *48*, 38.
8. Gopal Ji; Shukla, SK.; Dwivedi, P.; Sundaram, S.; Ebenso, EE.; Prakash, R. *Int. J. Electrochem. Sci.* **2012**, *7*, 12146.
9. Arockia selvi, J.; Rajendran, S.; Ganga Sri, V.; Amalraj, AJ.; Narayanasamy, B. *Port. Electrochim. Acta.* **2009**, *27*, 1.
10. Gopal Ji; Anjum, S.; Sundaram, S.; Prakash, R. *Corros. Sci.* **2015**, *90*, 107.
11. Rocha, JCD.; Gomes, JADCP.; Elia, ED. *Corros. Sci.* **2010**, *52*, 2341.
12. Abdallah, M. *Port. Electrochim. Acta.* **2004**, *22*, 161.
13. Mobin, M.; Khan, MA.; Parveen, M. *J. Appl. Polym. Sci.* **2011**, *121*, 1558.
14. Oki, M.; Charles, E.; Alaka, C.; Oki, TK. *Mater. Sci. Appl.* **2011**, *2*, 592.
15. Umoren, SA.; Solomon, MM.; Udosoro, II.; Udoh, AP. *Cellulose*. **2010**, *17*, 635.
16. Arukalam, IO.; Madufor, IC.; Ogbobe, O.; Oguzie, EE. *Chem. Eng. Commun.* **2015**, *22*, 112.
17. Rajeswari, V.; Kesavan, D.; Gopiraman, M.; Viswanathamurthi, P. *Carbohydr. Polym.* **2013**, *95*, 288.
18. Fiori-Bimbi, MV.; Alvarez, PE.; Vaca, H.; Gervasi, CA. *Corros. Sci.* **2015**, *92*, 192.
19. Fekry, AM.; Mohamed, RR. *Electrochim. Acta.* **2010**, *55*, 1933.
20. Sangeetha, Y.; Meenakshi, S.; Sairam Sundaram, C. *Int. J. Biol. Macromol.* **2015**, *72*, 1244.

21. Waanders, FB.; Vorster, SW.; Geldenhuys, AJ. *Hyperfine Interact.* **2002**, 139, 133.
22. Aghzzaf, AA.; Rhouta, B.; Steinmetz, J.; Rocca, E.; Aranda, L.; Khalil, A.; Yvon J.; Daoudi, L. *Appl. Clay Sci.* **2012**, 65, 173.
23. Alsabagh, AM.; Elsabee, MZ.; Moustafa, YM.; Elfky, A.; Morsi, RE. *Egypt. J. Pet.*, **2014**, 23, 349.
24. Hussein, MHM.; El-Hady, MF.; Shehata, HAH.; Hegazy, MA.; Hefni, HHH. *J. Surfactants. Deterg.* **2013**, 16, 233.
25. Umoren, SA.; Banera, MJ.; Alonso-Garcia, T.; Gervasi, CA.; Mirifico, MV. *Cellulose*, **2013**, 20, 2529.
26. Ashassi-Sorkhabi, H.; Majidi, MR.; Seyyedi, K. *Appl. Surf. Sci.* **2004**, 225, 176.
27. Anejjar, A.; Salghi, R.; Zarrouk, A.; Zarrok, H.; Benali, O.; Hammouti, B.; Al-Deyab, SS.; Benchat, NE.; Saddik., R. *Res. Chem. Intermediat.* **2015**, 41, 913.
28. Gopiraman, M.; Selvakumaran, N.; Kesavan, D.; Kim, IS.; Karvembu, R. *Ind. Eng. Chem. Res.* **2012**, 51, 7910.
29. Cho, YW.; Jang, J.; Park, CR.; Ko, SW. *Biomacromolecules.* **2000**, 1, 609.
30. Chidiebere, MA.; Oguzie, EE.; Liu, L.; Li, Y.; Wang, F. *Ind. Eng. Chem. Res.* **2014**, 53, 7670.
31. Oguzie, EE.; Li, Y.; Wang, FH. *J. Colloid Interface Sci.* **2007**, 310, 90.

**A Monthly Journal**

**Publish your article in this journal**

Advanced Materials Letters is an official international journal of International Association of Advanced Materials (IAAM, [www.iaamonline.org](http://www.iaamonline.org)) published monthly by VBRI Press AB from Sweden. The journal is intended to provide high-quality peer-review articles in the fascinating field of materials science and technology particularly in the area of structure, synthesis and processing, characterisation, advanced-state properties and applications of materials. All published articles are indexed in various databases and are available download for free. The manuscript management system is completely electronic and has fast and fair peer-review process. The journal includes review article, research article, notes, letter to editor and short communications.

[www.vbripress.com/aml](http://www.vbripress.com/aml)

Copyright © 2016 VBRI Press AB, Sweden

Supporting information

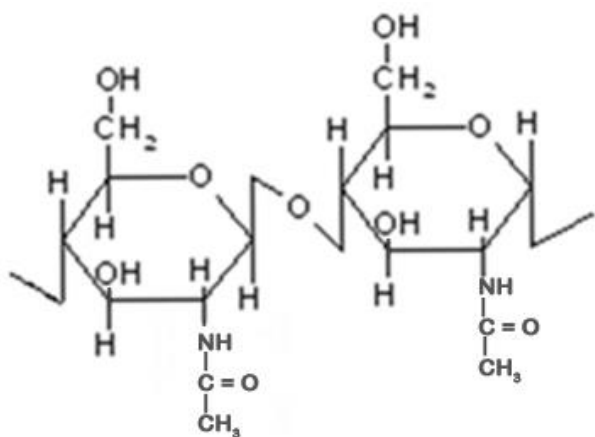


Fig. S1. Structure of Chitin.

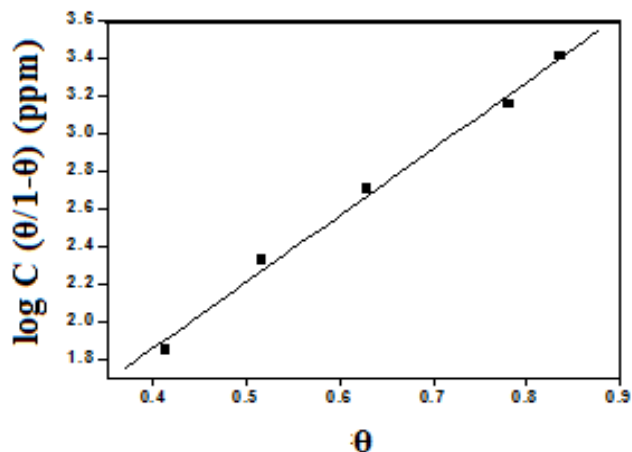


Fig. S2. Frumkin adsorption isotherm of WSC adsorbed on mild steel in 1 M HCl.

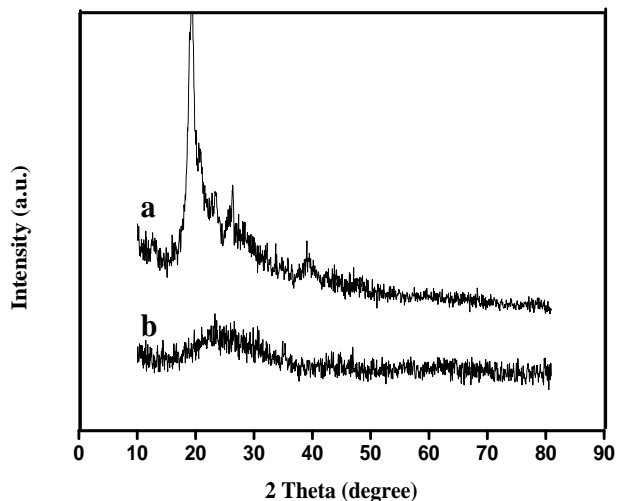


Fig. S3. XRD pattern for (a) chitin and (b) chitin adsorbed on mild steel in 1 M HCl.

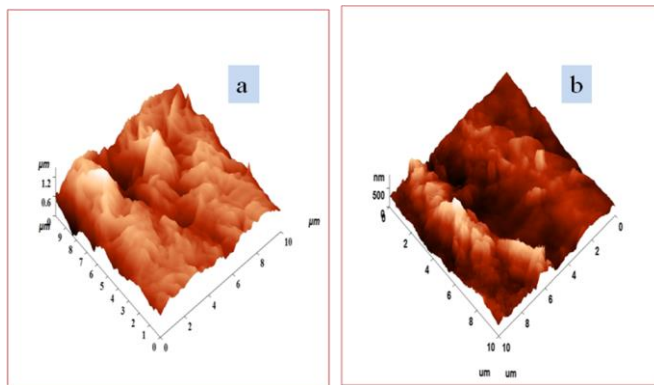


Fig. S4. AFM images of (a) uninhibited (b) inhibited mild steel specimens.

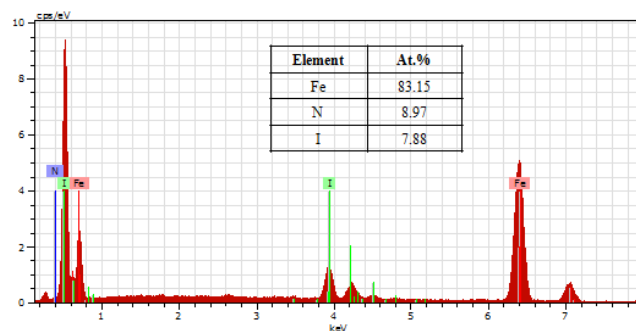


Fig. S5. EDX analysis of mild steel immersed in 1 M HCl in the presence of 500 ppm of WSC and 0.1 % KI.

Table S1. Thermodynamic parameters for mild steel in 1 M HCl in the presence of inhibitor at different temperatures.

Temperature (K)	$K_{ads}$ (mg litre <sup>-1</sup> )	$\Delta G_{ads}$ (kJ/mol)	$R^2$
303	1.55	-14.02	0.996
313	1.69	-14.87	0.991
323	1.69	-15.31	0.991

Table S2. Impedance parameters of mild steel in 1 M HCl in the absence and presence of different concentrations of WSC and WSC + KI.

Concentration (ppm)	$R_{ct}$ ( $\Omega$ cm <sup>2</sup> )	$C_{dl}$ ( $\mu$ F/cm <sup>2</sup> )	IE (%)
Blank	27.3	551	-
100	137.1	21.4	80.1
200	148.6	18	81.6
300	196.9	10.5	86.1
400	208.5	9.1	86.9
500	228.9	7.6	83.5
500+0.1% KI	301	4.6	90.9